AIAA 81-0670R

Ion Beam Texturing of Heat-Transfer Surfaces

P.K. Agarwal* and E. L. Park Jr.†
University of Mississippi, University, Miss.
and
A. J. Weigand‡
NASA Lewis Research Center, Cleveland, Ohio

Heat-transfer surfaces were textured by placing them perpendicular to the ion beam axis and centered on this axis. A low-sputtering-yield, seed material was located near the target at an angle to the ion beam axis. The ion beam simultaneously sputtered both the target and the seed material. The surface texturing was controlled by regulating the voltage, current density, and the time the ion beam was active. Nucleate boiling curves were obtained for textured copper surfaces, untreated copper surfaces, copper surfaces which had been polished, and surfaces which had been coated with a plasma deposited polymer. The data for the untreated surfaces were compared to the data obtained for the treated surfaces. The polished surfaces, the untreated surfaces, and the textured surfaces were found to exhibit progressively increasing boiling heat transfer characteristics indicating the importance of surface microgeometry. An indication that aging effects were dependent on surface microgeometry was also found.

Introduction

As a consequence of the recent energy crisis, it is becoming more important for effective methods of energy conservation to be developed. One method of conserving energy is to develop heat-transfer surfaces which are more efficient than those surfaces now in use. This investigation is concerned with this aspect of boiling heat transfer. A study of nucleate boiling of Freon 113 from copper surfaces with no surface preparation and surfaces prepared by ion beam texturing, polishing, ion beam texturing followed by coating with plasma deposited polymers, and polishing followed by coating with plasma deposited polymers was conducted. The nucleate boiling curves obtained for untreated copper surfaces were used for reference in interpretation of the effect of the surface preparations.

Because of the extensive literature which has been published concerning nucleate boiling in the last three decades, a complete discussion of previous work will not be presented here. If the reader requires background information he is referred to one of many review articles or textbooks that have been devoted to the nucleate boiling phenomena: Rohsenow,[1,2] Leppert and Pitts,[3] Hahne and Grigull,[4] and Frost.[5]

Experimental Equipment

Nucleate Boiling Apparatus

The experimental equipment that was utilized in the nucleate boiling portion of this investigation can be classified into five categories: the heat transfer test surface; the boiling chamber; the pressure control system; the heat source bundle; and the temperature measurement system. The apparatus used is similar to that used by Messina[6] for his study of boiling from photo-etched surfaces.

The heat transfer test surfaces consisted of copper (type 110) blocks machined according to the specifications shown in Fig. 1. The top end, which was in contact with the boiling fluid, was circular in shape with a diameter of 3.175 cm. The bottom end, which was in contact with the heat source bundle, was 3.81 cm in diameter. A groove 3.175-cm long and 0.236-cm deep was cut in the bottom end of the test section to provide a path for the thermocouples to exit from the apparatus. Three thermocouple wells were drilled in the groove as shown in Fig. 1. The depth of the holes was 0.9525 cm. The copper-constantan thermocouple wires were soldered in place with high temperature multicore solder (melting point 569 K). The boiling chamber (see Figs. 2 and 3) consisted of a 0.3048-m length of 15.24-cm nominal diameter thick-wall Pyrex pipe. The top of the chamber was a 1.27-cm thick aluminum plate which was attached to the Pyrex pipe by bolting the plate to a conical pipe flange. The plate-pipe interface was sealed with a flat Teflon gasket. The bottom of the chamber was a 2.8575-cm thick plate of solid Teflon with a 3.175-cm-diam hole machined through the center to admit the interchangeable heat transfer test surfaces. The Teflon plate had 12 holes drilled through it so that the plate could be fastened to a pipe flange. Two other holes in the Teflon plate had bolts screwed through them. These bolts extended well below the Teflon plate and were used to secure the heat source bundle and to

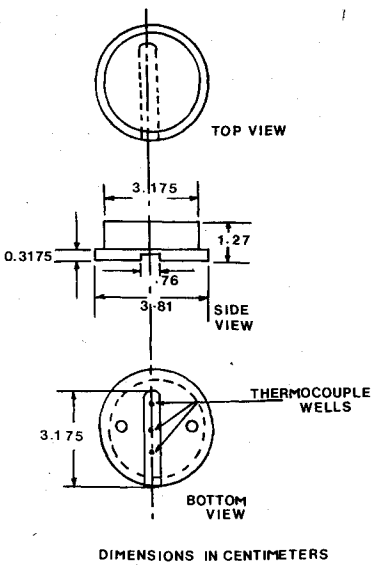

Fig. 1 Heat transfer surface.

Presented as Paper 81-0670 at the AIAA/JSASS/DGLR 15th International Electric Propulsion Conference, Las Vegas, Nev., April 21-23, 1981; submitted April 30, 1981; revision received Nov. 23, 1981.

*Research Fellow, Chemical Engineering Department.
†Former Chairman and Professor, Chemical Engineering Department, deceased.
‡Research Engineer.

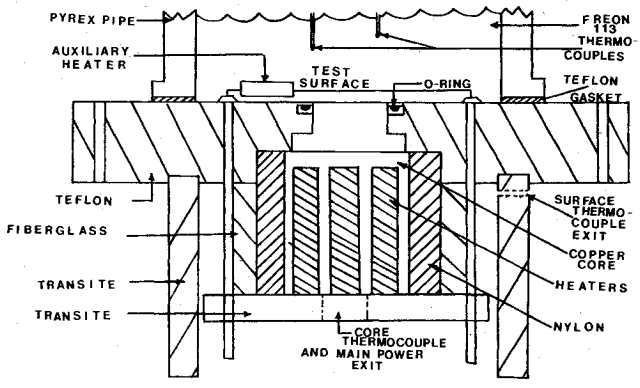

Fig. 2 Schematic diagram of the experimental equipment.

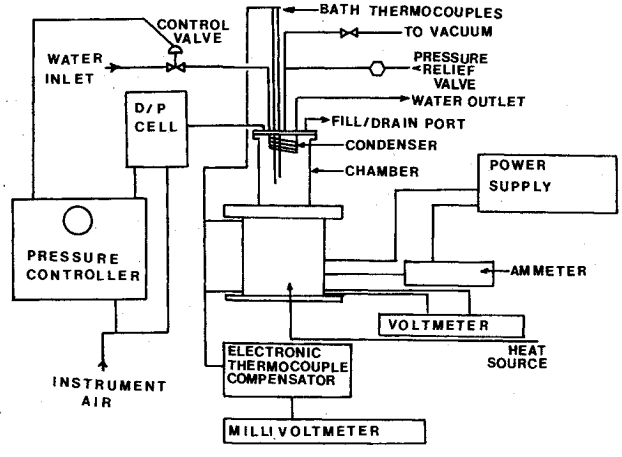

Fig. 3 Component diagram of the equipment.

serve as power leads for the auxiliary heat that was used to insure that the Freon 113 was at its saturation temperature throughout the experiment.

An o-ring (inserted as shown in the schematic diagram Fig. 2), was used to seal the interface between the heat transfer test surface and the Teflon plate.

The heat source bundle (see Fig. 2) consisted of three bayonet electrical heaters sheathed in a 5.08-cm-diam copper rod 7-cm long. The copper cylinder was covered with several layers of insulation to minimize heat losses. These layers of insulation have been identified in the schematic diagram, Fig. 2. The power to the bayonet heaters was furnished by a dc power supply. The power supplied was read using a 0-50 A ammeter and a 0-150 V voltmeter. Three thermocouples imbedded in the copper cylinder were used to monitor the temperature of the heat source bundle.

The pressure inside the boiling chamber (see Fig. 3) was sensed at the top of the vapor space through a port in the aluminum plate. The port was connected to the high-pressure side of a differential pressure cell; the low-pressure side was left open to the atmosphere. The pneumatic signal from the differential-pressure cell was transmitted to a proportional-integral pneumatic recorder controller that had been previously calibrated. The signal from the recorder controller operated an "air-to-close" control valve which controlled the cooling water flow to the boiling chamber condenser and, hence, the pressure inside the chamber.

The three thermocouples leading from the heater core, the three from the test surface, and the two from the pool were connected consecutively to the first eight terminals of a 23-position thermocouple switch. The output of the switch was wired to a thermocouple compensator whose output was a millivolt signal which referenced the thermocouple output to 0°C. The thermocouple signals were read with a digital

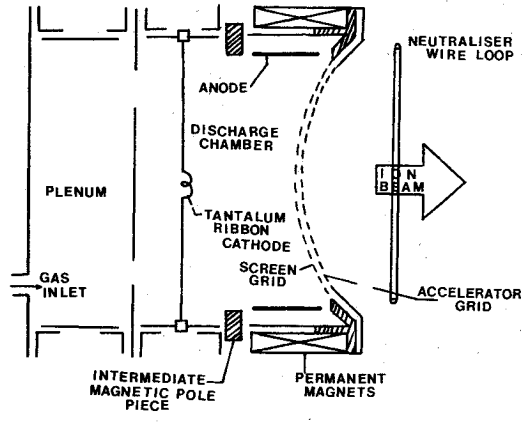

Fig. 4 Cross section of ion-beam source.

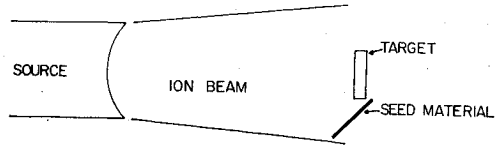

Fig. 5 Ion beam surface texturing with seed material.

millivoltmeter. The component systems and their interactions have been schematically represented in Fig. 3.

Ion Beam Texturing Apparatus

Most ion sources are cylindrical in design and typically are classified according to their beam diameters.[7] An 8-cm-diam ion source utilizing argon as the working gas was used to texture all the surfaces used in this investigation. The ion source operates in a vacuum system with pressures ranging from 1.3×10^{-3} to 4×10^{-4} Pa (1×10^{-5} to 3×10^{-7} Torr).

A schematic drawing of an 8-cm-diam source is shown in Fig. 4. The basic design of the ion source includes a ribbon cathode which, when heated, is the source of bombarding electrons used to ionize the working gas. The cathode is made of a triple-strand of 0.5-mm-diam, tantalum wire which is coated with a low-work-function material (BaO). The BaO aids in the electron emissions process. The electron emission is controlled by the amount of power applied to the cathode filament. The discharge chamber is the volume in which the cathode electrons ionize the working gas atoms. A concentric-cylinder anode, operating at approximately +40 V higher potential than the cathode, is used to attract electrons. A magnetic field, provided by six to eight 0.6-cm-diam permanent bar magnets equally spaced around the ion source, increases the bombarding electron path length through the discharge chamber. By extending the path length, the probability of ionization increases. The multiple aperture ion extraction system consists of two grids with concentric, circular holes.[8] The screen grid (adjacent to the discharge chamber) operates at a positive high voltage (300 to 2000 V), while the accelerator grid operates at a negative voltage (−200 to −1000 V). A neutralizer, which for this ion source is a heated loop of double strand, tantalum wire coated with BaO, provides electrons to neutralize the extracted ion beam. There is very little (approximately 1%) recombination of ions and electrons. This directed, slightly divergent, neutralized ion beam can then be used to sputter target material. Ion current densities from less than 0.1 to 1 mA/cm^2 are produced by the 8-cm-diam source. The maximum target area over which the ion current density is uniform (within 15% of maximum) is 12×12 cm^2 at a distance of 100 cm from the accelerator grid plane of an 8-cm-diam ion source.

The ion source is extremely easy to operate. The operator first turns on the cathode and neutralizer filaments. When

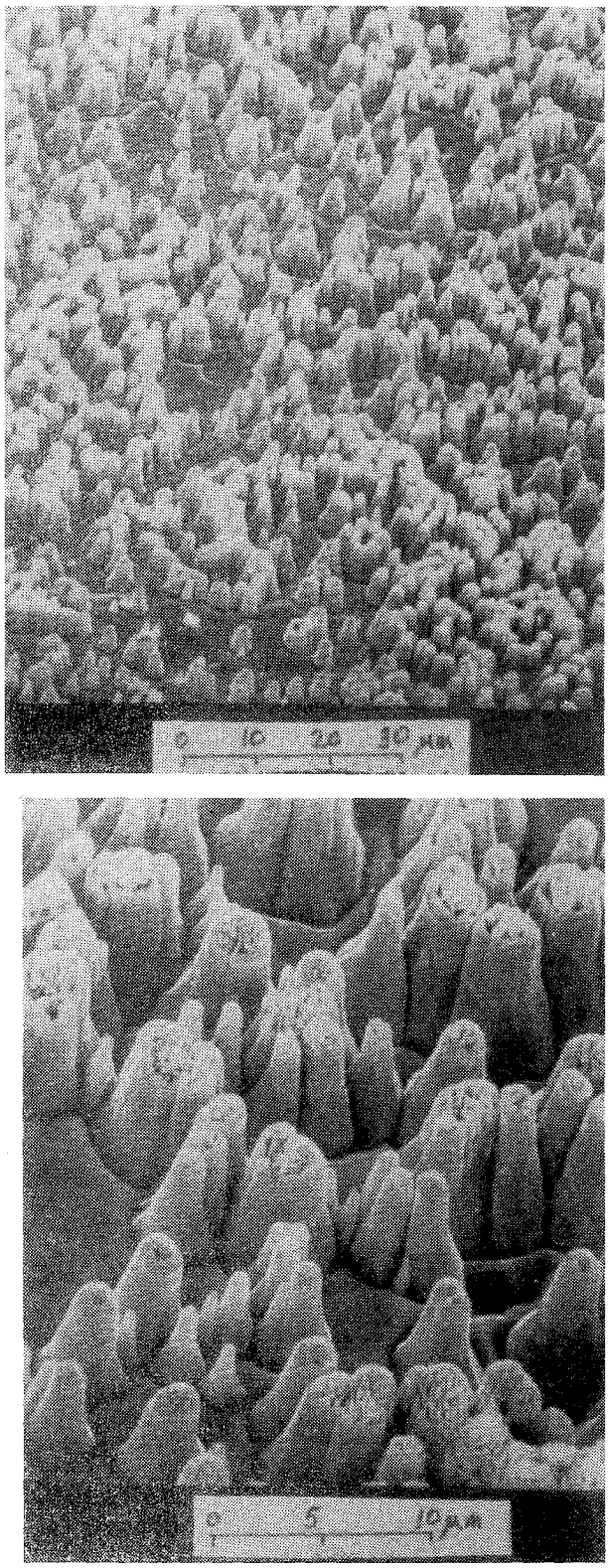

Fig. 6 Micrographs of ion beam textured surfaces.

they are heated to the proper level, the working gas flow is started. The flow can be regulated by a needle valve. The anode voltage is activated and a discharge is obtained. The two grid voltages are activated simultaneously which results in an ion beam. The screen grid voltage controls the ion beam energy. The ion beam current density is regulated by the anode current. Figure 5 shows the arrangement used to generate surface textures on most metals. The target is centered on the ion beam axis, and placed perpendicular to this axis 10 cm from the ion source. A low-sputtering-yield seed material is located in the proximity of the target and usually at a 30-45 deg angle with respect to the ion beam axis. The ion beam simultaneously sputters both the target and seed material. Some of the seed material is deposited on the target surface. Because the seed material has a low sputtering yield, each atom will prevent sputtering of target material behind it.[9] By adjusting the seed arrival rate, target temperature, and ion beam power, a variety of surface textures can be obtained.[10,11]

To generate the desired micron-size cones on the copper surfaces the ion source was operated for one hour at a positive high voltage of 1400 V, a negative voltage of -500, and a current density of 1.3 mA/cm^2. The seed material angle was 37 deg. The resulting surface morphology is shown in Fig. 6.

The polished surfaces were prepared, using the procedure outlined by Messina,[6] by sanding (using papers of roughnesses 240-600 grit) followed by mechanical polishing, and finally cleaning with acetone to achieve a close "mirror" finish.

For a discussion of the equipment used for the deposition of the polymers on the heat transfer surfaces the reader is referred to the work of Thompson and Mayhan.[12]

Discussion of Errors

Experimental errors in the investigation can occur in three types of measurements: temperature measurements, heat flux measurements, and pressure measurements. All thermocouple measurements were electronically compensated to 0°C and read on a digital millivoltmeter. This millivoltmeter was accurate to 0.02% of the 20-mV full scale range. At moderate to high fluxes, especially for polished surfaces, fluctuations in the readings (± 0.3 K) made it necessary to average the readings mentally, introducing some errors. In all cases, this error would be less than the fluctuations. Messina,[6] who used a similar kind of experimental setup, estimates the accuracy of his temperature measurements to be ± 0.3°C.

Calculated heat fluxes can involve errors of two types: 1) errors in measuring the input power to the heater core and 2) heat loss through the heat source bundle.

1) Input power: The main power supply voltmeter was accurate to ± 0.67% of the 150-V range and the ammeter was accurate to ± 1% of the 5-A range. The error in input power can be estimated to be ± 1.21%.

2) Heat loss: The heat losses can be estimated by considering heat loss in the radial direction through the surrounding insulation of nylon, fiberglass, air and transite; and heat loss through the bottom. The conduction heat losses through thermocouples and power leads may be neglected.

Heat loss in the radial direction may be calculated by steady-state conduction through composite cylinders and the bottom losses may be approximated by making use of a one-dimensional steady-state conduction through a plate model.

Messina[6] has made fairly rigorous calculations and analysis and concludes that combination of these errors introduces errors into the calculated surface heat flux of less than 5% for the entire nucleate boiling range. Since this apparatus is essentially the same as Messina's, it is felt that his maximum value of 5% error for heat loss is valid for this study.

The pressure in the system was always controlled to within ± 390 N/m^2. Messina[6] concluded that errors introduced by pressure fluctuations were insignificant. This has been corroborated during this investigation. The extremely good reproducibility found by Messina[6] and Warner[13] when the pressure was controlled within a narrow range of ± 390 N/m^2 was also apparent in this investigation.

Results

The nucleate boiling data collected during this investigation are shown graphically for the unprepared surfaces (Fig. 7), the ion beam textured surfaces (Fig. 8), and the polished surfaces (Fig. 9). The plasma deposited polymer coatings were found to have no appreciable effect on the nucleate boiling

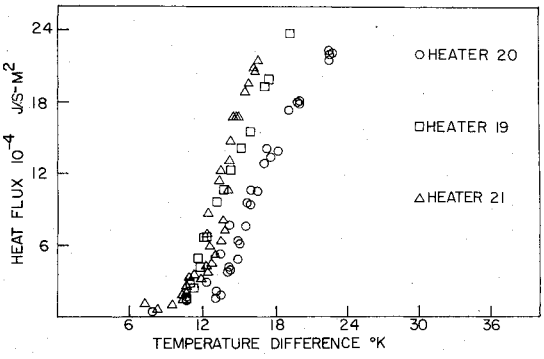

Fig. 7 Nucleate boiling from unprepared surfaces.

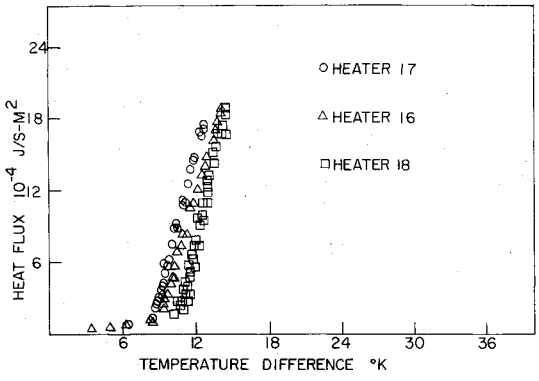

Fig. 8 Nucleate boiling from ion beam textured surfaces.

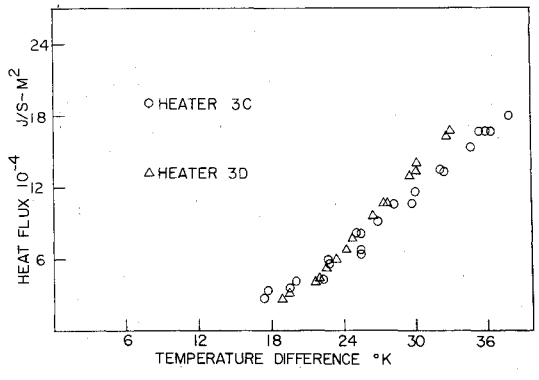

Fig. 9 Nucleate boiling from polished surfaces.

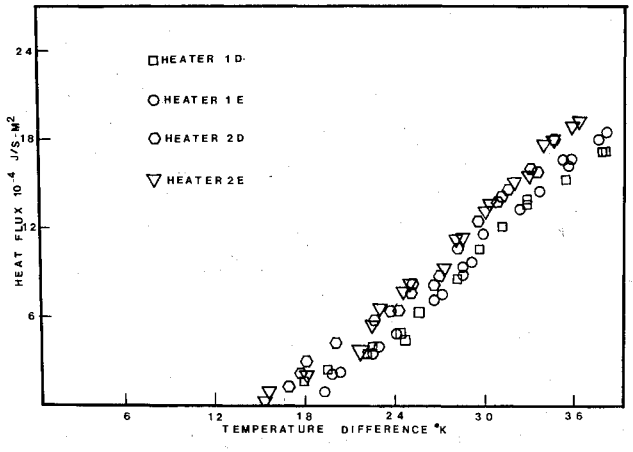

Fig. 10 Nucleate boiling from surfaces with polishing followed by plasma deposited polymer coatings.

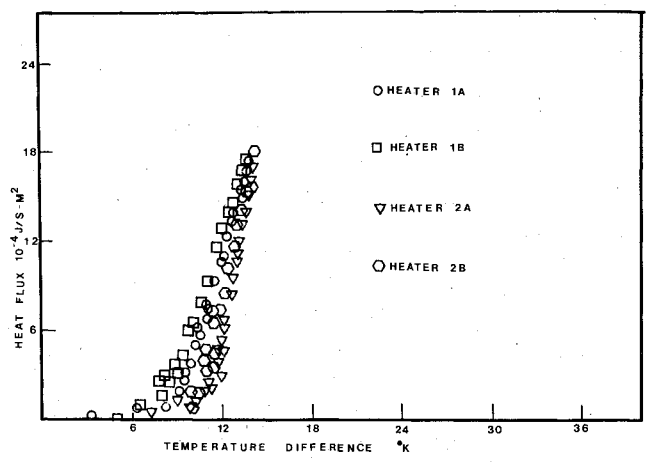

Fig. 11 Nucleate boiling from surfaces with ion beam texturing followed by plasma deposited polymer coatings.

curves generated; that is, coating a given surface with the polymer coatings did not change its nucleate boiling behavior (Figs. 10 and 11). The data collected fits reasonably well with Rohsenow's correlation for nucleate pool boiling.

The temperature differences used were calculated by averaging the readings from the three thermocouples located in the test surface. The surface area for heat transfer was computed as $\pi D^2/4$ where D is the circular diameter of the top end of the heat transfer surface (3.175 cm). The individual thermocouple readings were tabulated by Agarwal.[14]

Discussion of Results

The data from the heaters which had no surface preparation (heaters 19, 20, and 21) are shown in Fig. 7. The scatter in the data for various runs with heaters 20 and 21 demonstrate aging effects. No conclusion, however, can be drawn whether aging increases or decreases heat transfer as an increase was obtained with heater 21 and a decrease with heater 20.

Surface 19 was allowed to boil overnight near the critical heat flux and data were taken only after three burnouts had been induced. Reproducible results obtained with the first two runs indicate that at least one burnout is essential for removing aging effects. This confirms the findings of Porchey[15,16] and Montgomery.[17]

Patchwise boiling similar to that described by Gaertner[18] was observed on all untreated surfaces at low heat fluxes. The observed patches originated roughly from the same spots for a particular heater when different runs were conducted.

Temperature gradients along the heater surfaces were also observed. These temperature gradients increased with increasing heat flux. The gradients varied from almost zero to about 5°F. The gradients possibly can be explained by the uneven nucleation densities which are indicated by the patchwise boiling.

Ion beam texturing yields a surface which is characterized by a series of peaks covering the surface (see Fig. 6). It should be noted that the tops of the truncated peaks are porous and should be effective nucleation sites. The data from the ion beam textured surfaces (heaters 16, 17, and 18) are shown in Fig. 8. It should be noted that the nucleate boiling curves produced by the textured surfaces are to the left of all curves produced by the untreated surfaces. This shift to the left indicates that the texturing of the surfaces has enhanced the heat transfer. This finding is consistent with the work of Corty and Foust[19] and Kurihara and Myers[20] who found that the properties of the heat-transfer surface such as roughness and chemical composition have a profound effect on nucleate boiling behavior. The textured surfaces did not show aging effects and no patchwise boiling was observed on any of the heaters during data acquisition.

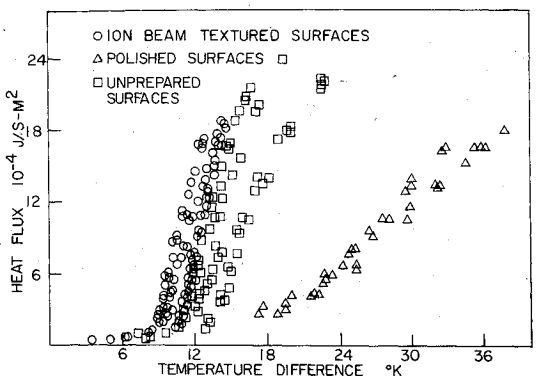

Fig. 12 Effect of surface topography on boiling.

The nucleate boiling data for the polished surfaces (heaters 3C and 3D) are presented in Fig. 9. It was noted that no patchwise boiling occurred on the polished surfaces; however, aging effects were noted to cause some scatter in the data. It was, also, observed that the polished surfaces took a much longer time to reach steady state than did the textured or untreated surfaces. The nucleate boiling curves for the polished surfaces were far to the right when compared to the untreated curves which indicates poor heat-transfer characteristics for the polished surfaces. This finding agrees with the data of Corty and Foust[19] and several investigators who followed them.

There was no indication of any effect due to the plasma deposited coatings which were applied to the polished (Fig. 10) and textured surfaces (Fig. 11). Plasma deposited polymer coating using CH_4 monomer was used on heaters 1A and 1B after texturing, and on heaters 1D and 1E after polishing. Plasma deposited polymer coating using $CF_2 = CF_2$ monomer was used on heater 2A and 2B after texturing, and on heaters 2D and 2E after polishing.

This data, seems to contradict the findings of Warner and Schade,[21] who found that coating a heat transfer surface with a plasma deposited polymer enhanced the heat transfer. However, both Schade and Warner postulated that the coating thickness must be thick enough to alter the topography of the surface before enhancement occurs. The coating on the surfaces used in this investigation were much thinner (less than 1-μ thick) than the coatings which enhanced the heat tranfer in Warner and Schade's investigations. These findings strongly indicate that the heat transfer in nucleate boiling is more dependent on the surface microgeometry than the surface chemistry of the surface if wetting is not a factor.

Figure 12 summarizes the results of this investigation. The curves indicate the area in which the nucleate boiling curves for a given type surface should fall. It is apparent that texturing aids heat transfer while polishing has the opposite effect.

To give the reader a feeling for the magnitude of the heat-transfer coefficients involved for the surfaces studied, the maximum and minimum values of the coefficients for each type of surface were calculated at a temperature difference of 13 K. These values of the heat-transfer coefficients for the polished surfaces were less than 142 J/s m^{2}K. The values of the heat-transfer coefficients for the untreated surfaces varied between 1820 and 7155 J/s m^2 K. The values of the heat-transfer coefficients for the textured surfaces varied between 8495 and 14,315 J/s m^2 K.

Conclusions

The data clearly indicates the importance of surface microgeometry in nucleate boiling heat transfer. If the data produced by the untreated copper surfaces (heaters 19, 20, and 21) are considered as reference curves, the nucleate boiling curve shifts towards the left (i.e., better heat-transfer characteristics) for textured surfaces and to the right for polished surfaces.

Aging effects were observed for untreated surfaces and for polished surfaces. No such effects were noticed for textured surfaces, which indicates aging may be a phenomena which is dependent on surface microgeometry.

Acknowledgments

We would like to acknowledge the following organizations which provided financial assistance during this investigation: Rotary International, which provided fellowship monies, and NASA Lewis, which provided financial support for the project.

References

[1] Roshenow, W.M., "Boiling," *Handbook of Heat Transfer,* McGraw-Hill Book Co., Inc., New York, 1973, p. 13-1.

[2] Roshenow, W.M. (ed.), *Development in Heat Transfer,* Massachusetts Institute of Technology Press, 1964, p. 169.

[3] Leppert, G. and Pitts, C.C., "Boiling," *Advances in Heat Transfer,* Academic Press, New York, 1964.

[4] Hahne, E. and Grigull, U. (eds.), *Heat Transfer in Boiling,* Academic Press, New York, 1977.

[5] Frost, W. (ed.), "Part II. Two Phase Phenomena," *Heat Transfer at Low Temperatures,* Plenum Press, New York, 1975, p. 89.

[6] Messina, A.D., "Effects of Precise Arrays of Pits on the Nucleate Boiling of Freon-113 from Flat Copper Surfaces at One Atmosphere Pressure," Ph.D. Thesis in Chemical Engineering, Univ. of Missouri, Rolla, Mo., 1978.

[7] "Ion Propulsion for Spacecraft," NASA Lewis Research Center, Cleveland, Ohio, 1977.

[8] Rawlin, V.K., Banks, B.A., and Byers, D.C., "Design Fabrication and Operation of Dished Accelerator Grids on a 30-cm Ion Thruster," NASA TM X-68013, 1972.

[9] Wehner, G.K. and Hajicek, D.J., "Cone Formation on Metal Targets During Sputtering," *Journal of Applied Physics,* Vol. 42, March 1971, pp. 1145-1149.

[10] Weigand, A.J., Meyer, M.L., and Ling, J.S., "Scanning-Electron Microscopy Observations and Mechanical Characteristics of Ion-Beam-Sputtered Surgical Implant Alloys," NASA TM X-3553, 1977.

[11] Hudson, W.R., "Ion Beam Texturing," NASA TM X-73470, 1976.

[12] Thompson, L.F. and Mayhan, K.G., "The Design Construction and Operation of an Inductively Coupled Plasma Generator and Preliminary Studies with Nine Monomers," *Journal of Applied Polymer Science,* Vol. 16, 1972, p. 2291.

[13] Warner, D.F., "Nucleate Boiling from Polymer Coated Surfaces," Ph.D. Thesis, Chemical Engineering Dept., Univ. of Missouri, Rolla, Mo., 1973.

[14] Agarwal, P.K., "Heat Transfer in Nucleate Boiling of Freon-113," M.S. Thesis, Chemical Engineering Dept., Univ. of Mississippi, University, Miss., 1979.

[15] Porchey, D.V., "A S.E.M. Surface Study of Nucleate Pool Boiling Heat Transfer to Saturated Liquid Nitrogen at Reduced Pressures from 0.1 to 0.9," Ph.D. Thesis, Chemical Engineering Dept., Univ. of Missouri, Rolla, Mo., 1970.

[16] Porchey, D.V., Park, E.L. Jr., and Mayhan, K.G., "A Scanning Electron Microscope Surface Study of Nucleate Pool Boiling Heat Transfer to Saturated Liquid Nitrogen," *Chemical Engineering Progress Symposium Series,* Vol. 68, 1972, pp. 162-171.

[17] Montgomery, R.T., "A Study of the Effect of Tube Bundle Geometry on the Nucleate Boiling Region of a Series of Hydrocarbon Liquids," Ph.D. Thesis, Chemical Engineering Dept., Univ. of Missouri, Rolla, Mo., 1969.

[18] Gaertner, R.F., "Distribution of Active Sites in the Nucleate Boiling of Liquids," *Chemical Engineering Progress Symposium Series,* Vol. 59, 1963, p. 56.

[19] Corty, C. and Foust, A.S., "Surface Variables in Nucleate Boiling," *Chemical Engineering Progress Symposium Series,* Vol. 51, 1955, p. 1.

[20] Kurihara, H.M. and Myers, J.E., "The Effects of Superheat and Surface Roughness on the Boiling Coefficient," *AiChE Journal,* Vol. 6, March 1960, p. 83.

[21] Schade, S.S., "A Study of the Effect of a Plasma Deposited Polymer Coating on the Nucleate Boiling Behavior of Freon-113," M.S. Thesis, Chemical Engineering Dept., Univ. of Missouri, Rolla, Mo., 1975.